Energy absorption in plasmas produced by intense 10-μm laser radiation

D. M. Villeneuve,[a), b)] G. D. Enright, M. C. Richardson, and N. R. Isenor[a)]

National Research Council of Canada, Division of Physics, Ottawa, K1A OR6, Canada
(Received 21 September 1978; accepted for publication 11 December 1978)

Results are presented of measurements made of the fractional absorption of short (~1 ns) intense (2×10^{14} W cm^{-2}) 10.6-μm laser radiation by plasmas produced from massive plane targets. Two complementary techniques were used: infrared light accounting and plasma calorimetry. The methods are shown to provide consistent results, demonstrating peak absorptions of up to 50%. The beam-polarization and irradiance-angle dependence of the absorption is consistent with a resonance absorption model. Plasma calorimetry also yields a detailed spatial distribution of the particle emission, while infrared calorimetry shows that the scattered laser light distribution is strongly dependent on the polarization of the incident laser beam.

PACS numbers: 52.25.Ps, 52.40.Db, 52.50.Jm

I. INTRODUCTION

One of the principal current problems in laser-fusion research is the determination of the mechanisms of absorption of the incident laser light. At the irradiance levels currently used, up to 10^{17} W cm^{-2} for 1-μm radiation and 10^{15} W cm^{-2} for 10-μm radiation, the plasma reaches temperatures such that absorption via inverse bremsstrahlung is no longer efficient.[1,2] However, in most experiments, for a variety of target configurations, considerable absorption does occur. As a consequence, a number of nonclassical absorption processes have been proposed.[3–10]

Recently, in experiments performed with intense short-pulse (~100 ps) Nd : glass laser systems in several laboratories, considerable evidence has accumulated which supports the view that, at these intensities, resonance absorption[11] on a steepened density profile plays an important, if not dominant, role in the interaction process. Direct absorption measurements made on thin bounded disk targets have identified the characteristic signatures of resonance absorption,[12] a sharp dependence on the irradiance angle for different orientations of the laser-beam polarization to the electron density gradient at the critical density n_c. The measurements showed peak absorption ($\lesssim 50\%$) occurring for p-polarized laser irradiation at angles of ~20°, in relatively good agreement with computations based on a predominant contribution (~90%) by resonance absorption on a steepened density profile having a scale length of the order of a wavelength.[13] Earlier studies of the polarization of the scattered laser light had implied scale lengths of this order,[14] and recently their direct measurement has been reported.[15] Similar polarization and irradiance-angle dependencies of the fractional absorption, also using 1.06-μm laser light, have been reported by Godwin *et al.*[16,17] In addition, observations of other characteristics of these plasmas, such as ion emission[18–20] and electron temperature,[21,22] have confirmed the sensitivity of the interaction to these parameters.

The characterization of the interaction of 10-μm radiation at similar values of $I\lambda^2$, where I is the laser intensity, is not so complete. However, the basic features of the interaction seem to be similar. Strong profile modification reduces the possible effects of inverse bremsstrahlung absorption and provides conditions suitable for resonance absorption. It is the purpose of this paper to describe a parametric study of the absorption characteristics of intense (~10^{14} W cm^{-2}) short (~1 ns) 10.6-μm laser pulses by plasmas produced from plane solid targets.[23] This has been accomplished using two independent complimentary techniques, infrared light energy accounting and direct plasma calorimetry. To within experimental error, the two techniques are in agreement. The absorption has been studied as a function of focus position, irradiance angle, beam polarization, power density, and to some extent, target material. In addition, the use of discrete plasma and infrared calorimeters has permitted the gross features of the ion blowoff energy distribution and the scattered laser light distribution to be characterized.

II. EXPERIMENTAL CONDITIONS

The experiments reported here were performed with one arm of the two-beam COCO-II CO_2 laser system. This system, which utilized an actively mode-locked oscillator and a number of uv preionized atmospheric-pressure CO_2 amplifier units, has been described in detail elsewhere.[24] Due to saturation effects in the amplifier chain and the use of a number of saturable absorber cells in the beam line, the approximately-Gaussian-shaped pulse emanating from the oscillator is considerably modified during amplification. Initial investigations using a picosecond resolution linear upconversion technique[25] indicate that the pulse has a rise time typically of ~400 ps and a falltime of 800–1000 ps. An on-line prepulse monitoring scheme is capable of detecting levels of prepulse > 50 μJ, and prelase, due to amplified

[a)]Department of Physics, University of Waterloo, Waterloo, Ont., Canada.
[b)]Work performed in partial fulfilment of a M.Sc. degree for the University of Waterloo.

 0021-8979/79/063921-07$01.10

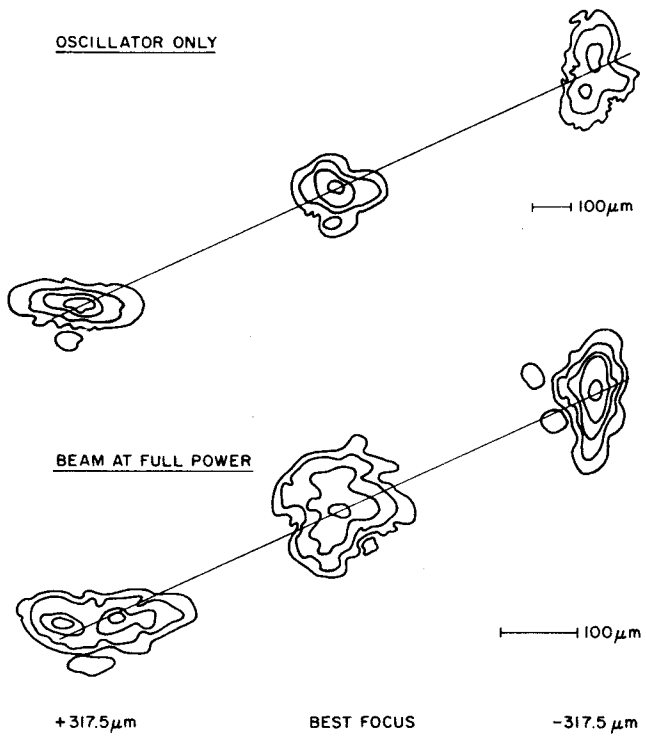

FIG. 1. Isoenergy contours of the focal spot distribution. Each contour step represents a factor of 2.

spontaneous emission, > 50kW. The pulse contrast ratio was $\sim 10^6$. The 80-mm-diam approximately-diffraction-limited beam was focused onto plane-polished Al targets in a vacuum of 5×10^{-5} Torr by an $f/2.5$ 20-cm focal length off-axis parabolic mirror. Maximum energy deliverable on target in these experiments was ~45 J.

In investigations of this nature, a precise knowledge of the intensity distribution in the focal region is required. In the present case, the focal spot size is limited by imperfections in the focusing mirror, and has a half-energy diameter of $\sim 110\,\mu$m and a half-intensity diameter of 75 μm.[26] The variation of the intensity distribution of the laser beam in the focal region is shown in Fig. 1. It can be seen that, although the beam distribution near focus is basically circular, at distances of several hundred microns on either side of focus the energy distribution is irregular in shape and contains several local intensity maxima. Thus, intensities of up to $\sim 2.4\times 10^{14}$ W cm^{-2} were deliverable on target with prepulse radiation levels of $\lesssim 2\times 10^8$ W cm^{-2}. Under these conditions, picosecond visible light interferometry[27] detected no plasma with electron density $> 10^{18}$ cm^{-3} on the surface of the target prior to irradiation by the laser pulse.

Although this paper describes primarily the absorption characteristics of plasmas produced by the irradiation of plane massive targets by intense nanosecond-duration CO_2 laser pulses, other characteristics of the interaction under identical conditions have been studied and have direct bearing on these investigations.

Picosecond interferometric investigations have characterized the development of the electron density distribution throughout and following the incidence of the laser pulse on target.[27] They show clear evidence of profile modification due to ponderomotive effects. A steepened density profile is observed even at moderate laser intensities ($\sim 10^{13}$ W cm^{-2}).[25] The plasma density has a scale length of $\sim 10\,\mu$m, extending from $0.2n_c$ ($n_c = 10^{19}$ cm^{-3}) to a density approximately equal to that for equilibration between radiation and plasma kinetic pressures ($\sim 7n_c$ for incident intensity of 2×10^{14} W cm^{-2}).[25]

Studies of the x-ray emission from the plasma indicate, both from line-ratio measurements and from bremsstrahlung continuum analysis,[28,29] plasma temperatures T_c of 300–400 eV behind this density step. However, examination of high-energy continuum emission identified a nonthermal electron component in the plasma which may be characterized by a hot electron temperature T_H that scales as $T_H \propto (I\lambda^2)^{\sigma}$, where σ is in the range 0.25–0.41, depending on target material.[29] These experimental results agree closely with the predictions of particle code simulations of the interaction based on resonance absorption at a steepened density profile.[30] Further evidence that strong resonant fields exist in the absorption region can be deduced from the appearance of an integral series of harmonics of the fundamental laser frequency in the backscatter and sidescatter infrared emission.[31,32]

Studies of the ion emission from plasmas produced by laser intensities in the range 10^{12}–10^{14} W cm^{-2} have also been made using charge collectors.[33] As in previous investigations, a component in the collector's signal resulting from superthermal ions of energy up to ~500 keV was observed in addition to that arising from the expanding plasma. Studies made with a number of charge collectors placed at various angles from the target normal indicate that the bulk of the superthermal ion component is emitted in a narrow cone of half-angle of ~10° about the target normal. However, comparative studies with a number of different designs of charge collectors have shown that the shape of the current signal

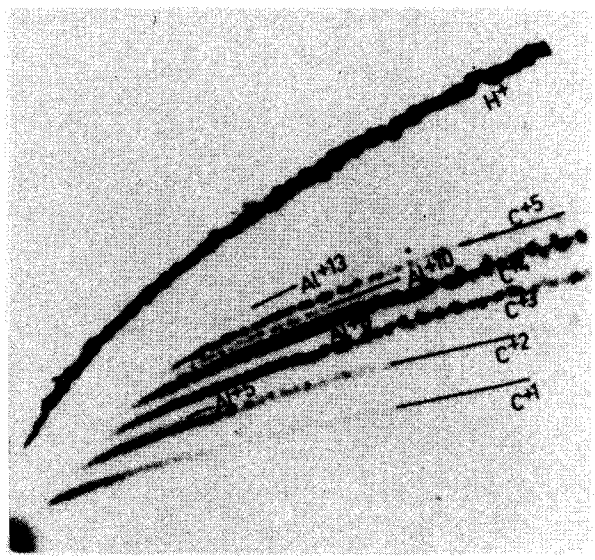

FIG. 2. Thomson parabola traces of fast ion emission from Al target irradiated with a 10.6-μm pulse of intensity $\sim 10^{14}$ W cm^{-2}. The traces correspond to energies in the range 20–200 keV.

corresponding to a particular ion flux is highly dependent on the electrode structure of the detector. Thus, the difficulty in estimating the secondary emission effects[34] which give rise to these variances precluded the use of charge collectors for the determination of a reliable ion energy spectrum. A Thomson parabola ion spectrograph[35] is currently being used to analyze the ion energy spectrum.[36] A typical record of the fast ion emission from the Al targets utilized in these studies is shown in Fig. 2. It can be seen that the fast ion emission contains carbon and hydrogen species, most likely due to contamination of the target surface by vacuum pump oil.

III. CHARACTERIZATION OF ABSORPTION

A. Measurements by laser-light accounting

The laser energy incident on the target (E_i) is converted into several forms during the interaction. This can be represented as the sum of a number of components as $E_i = E_a + E_b + E_s + E_x$, where E_b, E_s, and E_x are, respectively, the energy found in the backscattered radiation, in the diffusely scattered radiation, and in the short-wavelength plasma emission. Since, for the interactions described here, $E_x/E_i \ll 1\%$,[28] the fractional absorbed energy (E_a/E_i) may be approximated by $E_a/E_i = 1 - (E_b + E_s)/E_i$. Thus, careful bookkeeping of the scattered infrared radiation can be used to estimate the fractional absorption. This approach has been adopted in previous 1-μm laser investigations, utilizing box calorimeters,[12] calibrated photodetectors,[14,37] and 2π or 4π collecting optics[16,17] to measure the scattered light. Such detailed diagnostics have not yet been published for 10-μm interaction experiments. To this end, 2π infrared collecting optics were used in the present investigations to determine the laser energy diffusely scattered from the plasma. Following an approach first used by Godwin *et al.* in Nd : glass laser investigations,[16] a 2π ellipsoidal mirror was positioned about the target as shown in Fig. 3. The ellipsoid, which had a major radius of $a = 62.5$ mm, a minor radius of $b = 50$ mm, and an ellipticity of $\epsilon = 0.6$, was fabricated of stainless steel, hand polished, and gold coated, with a measured reflectivity of 85%. It was positioned so that the target was situated at one of its principal foci, and a calibrated 50-mm-diameter pyroelectric detector was positioned immediately behind the target. This detector, and the pyroelectric detector monitoring the collimated backscatter, were calibrated relative to the incident laser energy detector, and hence the measured fractional absorption was independent of the absolute calibration of any one detector. The targets for these investigations were 3-mm-diam polished Al cylinders 4 mm long, supported by long thin 1-mm steel stalks attached rigidly to a 10-target carrousel. A conical hole through the ellipsoidal mirror at an angle of 21° to the mirror and target axis permitted entry of the laser beam and measurement of the collimated backscattered radiation.

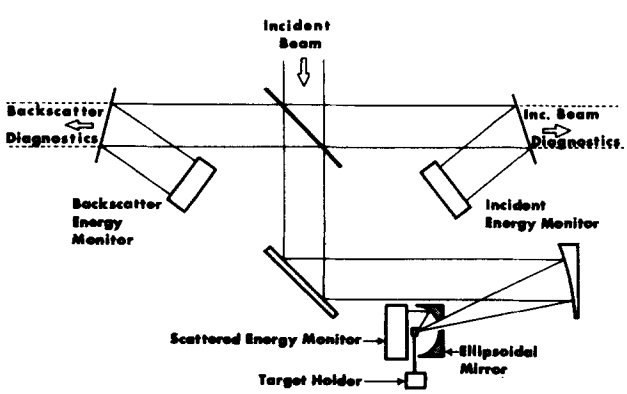

FIG. 3. Experimental arrangement for 2π infrared light collection.

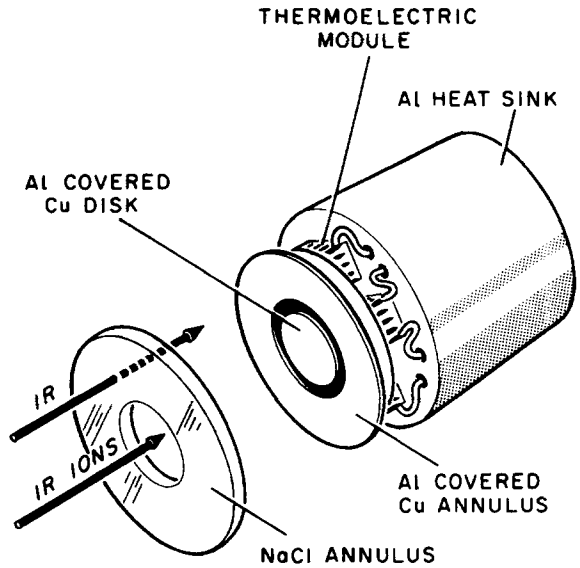

FIG. 4. Configuration of plasma calorimeters.

B. Plasma calorimetry measurements

The fractional absorption was also measured using an alternative approach. Although charge collectors have been used for determining absorption, the lack of knowledge of their response to high-energy ions throws suspicion on the accuracy of such determinations. On the other hand, plasma calorimeters, which depend upon thermal detection of particle emission from the plasma, do not have such drawbacks.

In these investigations, a number of differential calorimeters of the type shown schematically in Fig. 4 were used. They were developed from an original design by Gunn and Rupert.[38] Basically, each calorimeter is comprised of a central Al-coated Cu disk, which is exposed to all emission from the plasma (particles, x-rays, and scattered laser light), and a concentric annular disk of similar construction which is permitted to record only infrared radiation. This is achieved through the use of an annular NaCl window which stops all plasma emission except infrared radiation. The temperature rise in the two absorbers is detected with the use of thermoelectric modules bonded between the absorber and an Al heat sink. Thus, after accounting for the reflective losses of the annular NaCl window, the difference in the two signals represents a measure of the energy in all ion species, electrons, neutrals, and x-rays. The difference signal (< 1 mV), amplified and recorded on a chart recorder, has an initial rise time of 0.5 s, followed by a falltime of ~ 60 s, thus circum-

venting high-frequency noise effects. Extrapolation of the exponential decay to zero time gives an estimate of the peak difference signal.

Each calorimeter was constructed to facilitate individual calibration. A $\frac{1}{8}$-W resistor was permanently located inside the central circular Cu disk. Thus, the calorimeter could be calibrated simply by discharging a capacitor having a known storage energy through the resistor. This procedure could be effected easily before and after each experimental run while the calorimeter was in position, under vacuum in the target chamber. The accuracy and long-term stability of the calibration was found to remain constant within 2%.

Six of these calorimeters were deployed about the target in either the vertical (V) or horizontal (H) plane at distances ~ 25 cm, each subtending a solid angle of 0.045 sr. The spatial distribution of the ion blowoff was then studied as a function of laser intensity, beam polarization, and irradiation angle. Some typical results are shown in Figs. 5 and 6. At low angles of incidence ($\sim 20°$) the ion blowoff distribution is fairly symmetric about the target normal for both the s- and p-polarized laser radiation. Although the general form of the distribution changes little with laser intensity, there is markedly more absorption for p- polarized than for s-polarized radiation. However, as the angle of irradiance is increased, the peak of the ion distribution skews away from the target normal towards the irradiation axis. Although the amount of skew in the horizontal plane did not appear to be intensity dependent, there was some shot-to-shot variation in the shape of the ion distribution.

In order to determine the total plasma energy, these distributions were graphically integrated. The complex form

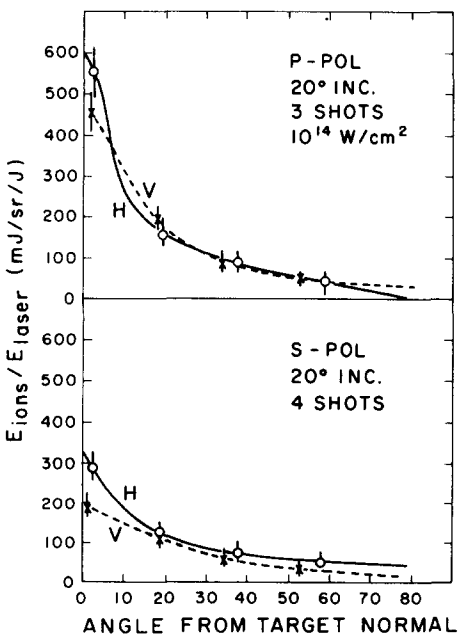

FIG. 5. Angular distribution of energy in plasma blowoff from Al targets with laser intensities of 5×10^{13} to 10^{14} W cm^{-2} at 20° irradiance angle. The data show the distribution in the horizontal (H) and vertical (V) planes and are normalized to the incident laser energy. P polarization corresponds to the E vector lying in the plane of incidence.

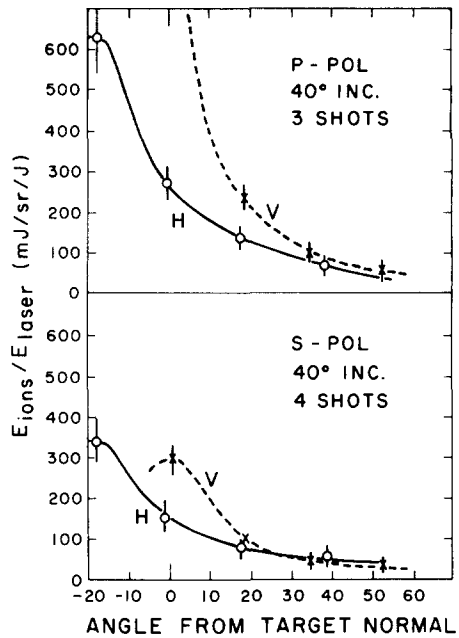

FIG. 6. Angular distribution of energy in plasma blowoff from Al targets with laser intensities of 5×10^{13} to 10^{14} W cm^{-2} at 40° irradiance angle.

of the distribution for high irradiance angles introduced some error into these measurements; the overall error in the absorption is estimated to be 15%.

C. Total absorption measurements

The total fractional absorption, deduced from both infrared light accounting and plasma calorimetry, was studied as a function of laser intensity, beam polarization, irradiance angle, and focus position.

In general, peak absorption values of 50% were obtained for small laser irradiance angles and p-polarized incident radiation. No intensity dependence within the range from 5×10^{12} to 5×10^{14} W cm^{-2} was evident, and within the limits of measurement, no clear dependence on focus position could be deduced. These are substantiated by similar measurements made at LASL,[39] where, in addition, no strong dependence of the fractional absorption on target material was discernable.

However, as can be seen from Fig. 7, there is a measurable difference in absorption between s- and p-polarized light at different irradiation angles. Although there is considerable scatter in the data, two general trends are evident. First, for a particular irradiance angle, absorption of p-polarized radiation is consistently higher than for s-polarization. In addition, it can be seen that in the range 10°–30°, the absorption of p-polarized radiation falls off sharply, while there is only a small decrease in absorption for s-polarized radiation. The dependence of the absorption on irradiance angle and beam polarization and its lack of dependence on laser intensity would be expected assuming a resonance absorption model. However, the results of Fig. 7 lack the clarity of the signatures of resonance absorption to be expected from plane-wave illumination of a stationary plasma profile. This is hardly surprising since, in the present investigations, low f-

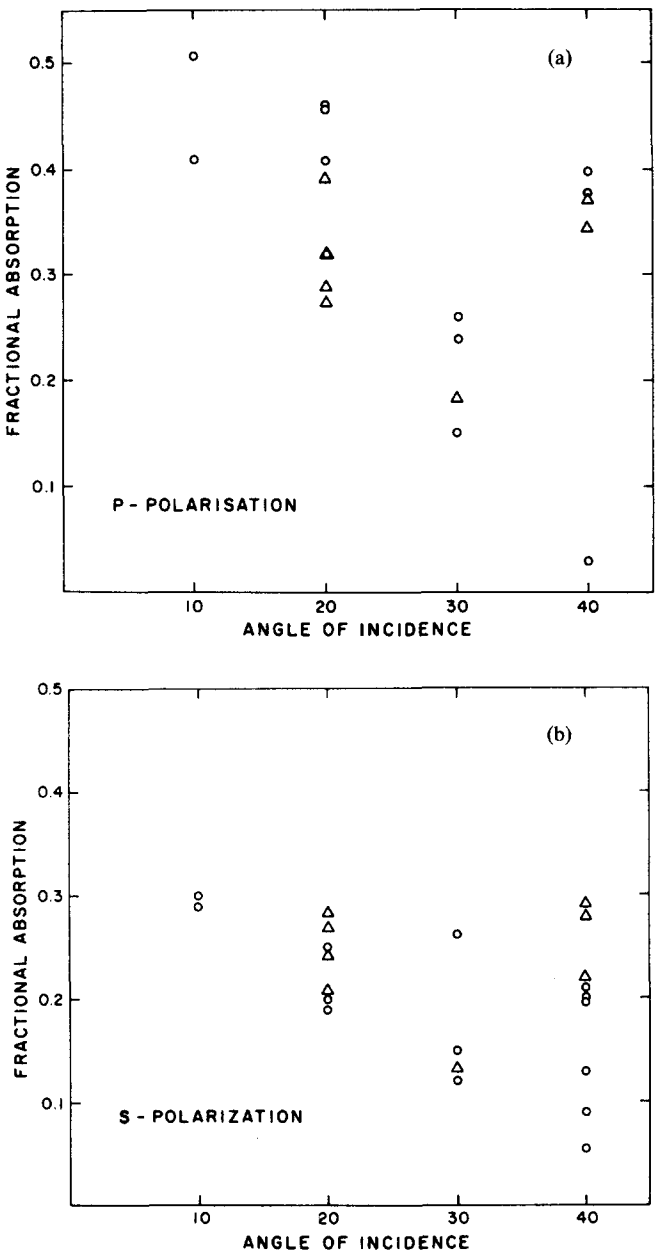

FIG. 7. Fractional absorption deduced by (i) infrared accounting (○) and (ii) plasma calorimetry (△) for (a) *p*-polarized and (b) *s*-polarized incident radiation for laser intensities in the range 10^{13}–10^{14} W cm^{-2}.

number focusing optics were utilized, and thus the large focal cone (20°) included a wide range of incident angles. In addition, for the 1-ns-duration pulses employed, the effects of hydrodynamic motion during the interaction cannot be ignored. Finally, recent direct evidence for the formation of deep density craters has been obtained for the conditions described here.[40] Thus, a model of the interaction based on resonance absorption must take into account these factors before closer agreement can be expected.

IV. DISTRIBUTION OF SCATTERED INFRARED RADIATION

Measurements of the angluar distribution of laser light scattered from the plasma has been recognized in investiga-

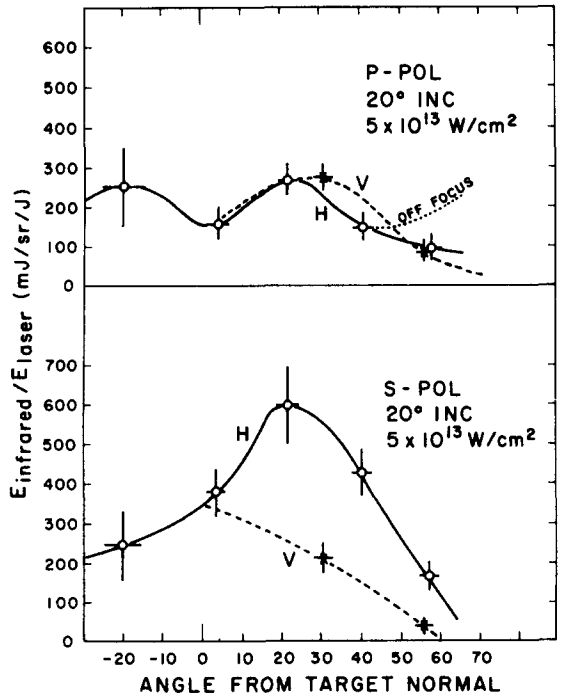

FIG. 8. Horizontal (H) and vertical (V) angular distributions of scattered infrared radiation for *p*- and *s*-polarized incident radiation, normalized to the incident laser energy.

tions with 1-μm lasers as a useful diagnosis of absorption processes in the interaction region.[14,37] However, the relative insensitivity of infrared detectors has made similar measurements with CO_2 laser-produced plasmas difficult. In the present investigations, a differential infrared calorimeter, modeled on a device previously developed for 1-μm investigations,[38] was employed. This calorimeter utilized thermoelectric modules similar to those embodied in the ion calorimeters, and consisted of two blackened absorbing disks, one shielded by an NaCl window to prevent the transmission of particle and x-ray emission and the second shielded from all plasma emission to provide a reference signal. A recording system similar to that utilized for the plasma calorimeters was used.

A number of these calorimeters were placed at various positions about the target in the vacuum chamber. The distribution of scattered infrared radiation was then investigated as a function of laser power, irradiation angle, and beam polarization. Typical infrared distributions in the vertical and horizontal planes for *p*- and *s*-polarized incident light are shown in Fig. 8 for a laser intensity of 5×10^{13} W cm^{-2} and an irradiance angle of 20°. The laser beam is incident from an angle of $-20°$ and the datum at that angle represents the collimated backscatter energy measured through the focusing optics. It can be seen that there is a striking difference between the cases for *p*- and *s*-polarized light. The distribution for *s*-polarization peaks in the specular direction at $+20°$ in the horizontal plane with an angular width of $\sim 30°$.

As can be seen, for *p*-polarized incident laser light the laser light is not scattered solely in the specular direction. In addition, whereas the angular distribution for *s*-polarized

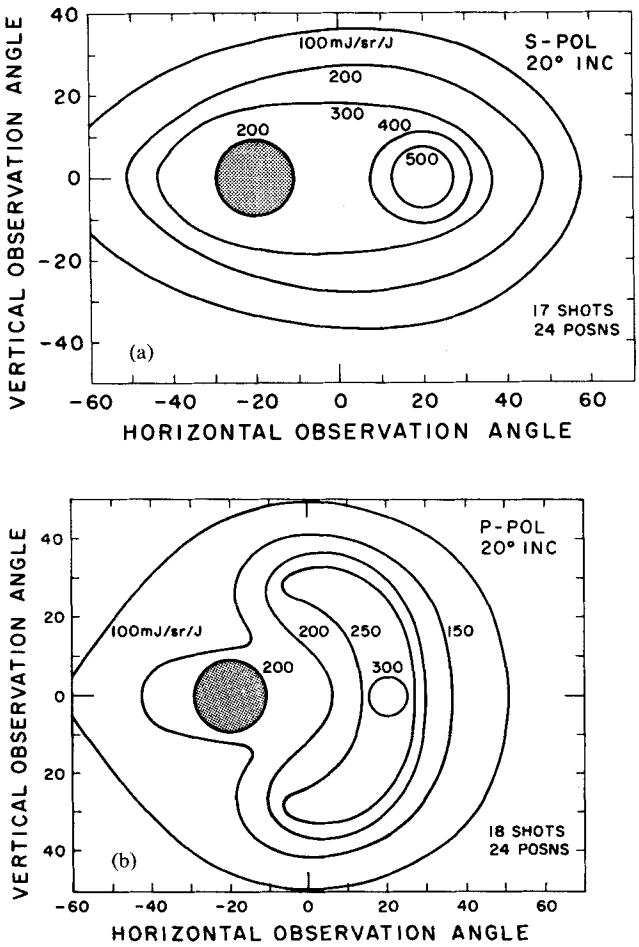

FIG. 9. Isoenergy contours of the scatter infrared radiation, normalized to the incident laser energy for laser intensities of 5×10^{13} to 10^{14} W cm^{-2} for (a) *s*-polarized incident light and (b) *p*-polarized incident laser light.

light was not found to be particularly sensitive to focus position, for *p*-polarized light a greater fraction of light was scattered at high angles in the out-of-focus positions. The anomalous character of the distribution for *p*-polarized light is more evident in Fig. 9. This shows the normalized isoenergy contours of the scattered light distributions, viewed normal to the target surface. The laser beam is incident at $-20°$ on the left-hand side of each distribution and the shaded areas represent the normalized collimated backscattered radiation, typically $\sim 5\%$ of the incident energy. These two distributions were obtained from a number of shots at approximately constant laser intensity ($\sim 10^{14}$ W cm^{-2}) utilizing six calorimeters placed at various positions relative to the target. Integration of these distributions yields an absorption of $\sim 40\%$ for *p*-polarization and $\sim 25\%$ for *s*-polarization, consistent with the values determined from the other two methods. It can be seen that in the case of *p*-polarization, much of the laser light is scattered in a crescent-shaped distribution, whose width remains similar to that of the specularly scattered light, even at high azimuthal angles.

A definitive explanation for the character of this distribution remains to be found. However, it is clear that any description will be significantly dependent on the general topography of the plasma surface and its temporal development during the laser pulse. This is especially true in the case of resonance absorption, which is governed by the steepness of the electron density profile through n_c and the direction of the density gradient. Although there is strong evidence for the existence of a steepened density profile in the plasmas produced off solid targets by nanosecond CO_2 laser pulses,[27] it seems now, in the light of more recent results,[40] that the picture is somewhat more complex. It appears from these results that at the intensities attained in these experiments (10^{14} W cm^{-2}) a deep density crater, having a diameter comparable to the focal spot diameter, is formed early in the development of the plasma. Thus, the detailed morphology of this crater, particularly the density gradient on its inside wall, would strongly affect the overall absorption and also have significant influence on the distribution of scattered laser light. As a consequence, the distributions of scattered laser light for *p*- and *s*-polarized laser light observed in these experiments may well be a general manifestation of the localized conditions for resonance absorption existent on the surface of the plasma. However, the influence and extent of other effects, such as a localized stimulated scattering or simple refractive effects in the plasma arising from the use of targets of infinite extent, have yet to be determined. In addition, it must be recognized that all these measurements are time integrated and therefore do not detect any possible temporal changes in the scattered light distribution.

V. CONCLUSIONS

The measurements presented above, together with interferometric,[27,40] high-harmonic,[31,32] and x-ray continuum data,[28,29] help to establish a consistent picture of intense 10-μm laser-plasma interaction. At intensities of $> 10^{13}$ W cm^{-2}, radiation pressure produces a steep gradient in the critical density region, thus inhibiting absorption through inverse bremsstrahlung. The angular dependence of fractional absorption as a function of beam polarization lends strong support to the contention that resonance absorption is the dominant absorption mechanism. However, several factors indicate that a simple model based on resonance absorption on a one-dimensional steepened density profile at the critical surface is not sufficient. Anomalously high absorption is observed for both *s*-polarized radiation and for normal incidence for both 1- and 10-μm laser light. This has previously been attributed to small-scale density rippling[13] or ion acoustic turbulence.[10] Although these processes may well be present, it is clear that these features of absorption could be accounted for by the existence of a density well or crater in the absorption region. Such a structure has been recently identified in these plasmas.[40] Thus, at the intensities considered here, the idealized conditions for *p*- or *s*-polarized interaction never exist. Rather, the existence of a density well created conditions suitable for resonance absorption for any orientation of the electric field vector in the incident beam.

ACKNOWLEDGMENTS

The authors wish to acknowledge useful discussions with R. Godwin, V. Cottles, V. Rupert, and K. Manes. They

also wish to thank G.A. Berry, P. Burtyn, R.W. Sancton, and Y.P. Lupien for their considerable technical support throughout the course of these investigations.

[1]J. Dawson, P. Kaw, and B. Green, Phys. Fluids **12**, 875 (1969).
[2]W.L. Kruer, *Progress in Lasers and Laser Fusion*, edited by B. Kursunoglu, A. Perlmutter, and S. Widayer (Plenum, New York, 1975), pp. 5–26.
[3]W.L. Kruer and J.M. Dawson, Phys. Fluids **15**, 446 (1972).
[4]C. Yamanaka, T. Yamanaka, T. Sasaki, K. Yoshida, and M. Waki, Phys. Rev. A **6**, 2335 (1972).
[5]J.J. Thomson, R.J. Faehl, W.L. Kruer, and S.E. Bodner, Phys. Fluids **17**, 973 (1974).
[6]H.H. Klein and W.M. Manheimer, Phys. Rev. Lett. **33**, 953 (1974).
[7]D.W. Forslund, J.M. Kindel, K. Lee, E.L. Lindman, and R.L. Morse, Phys. Rev. A **11**, 679 (1975).
[8]A.T. Lin and J.M. Dawson, Phys. Fluids **18**, 1542 (1975).
[9]W.M. Manheimer, D.G. Colombant, and R. Flynn, Phys. Fluids **19**, 1354 (1976).
[10]W.M. Manheimer, D.G. Colombant, and B.H. Ripin, Phys. Rev. Lett. **38**, 1135 (1977).
[11]V.L. Ginzburg, *The Propagation of Electromagnetic Waves in Plasmas* (Pergamon, New York, 1964), Chap. 4.
[12]K.R. Manes, V.C. Rupert, J.M. Auerbach, P. Lee, and J.E. Swain, Phys. Rev. Lett. **39**, 281 (1977).
[13]J.J. Thomson, W.L. Kruer, A.B. Langdon, C.E. Max, and W.C. Mead, presented at the Anomalous Absorption Conference, Ann Arbor, Mich., 1977 (unpublished).
[14]D.W. Phillion, R.A. Lerche, V.C. Rupert, R.A. Haas, and M.J. Boyle, Phys. Fluids **20**, 1892 (1977).
[15]D.T. Attwood, D.W. Sweeney, J.M. Auerbach, and P.H.Y. Lee, Phys. Rev. Lett. **40**, 184 (1978).
[16]R.P. Godwin, C.G.M. van Kessel, J.N. Olsen, P. Sachsenmaier, R. Sigel, and K. Eidmann, Z. Naturforsch. A **32**, 1100 (1977).
[17]R.P. Godwin, P. Sachsenmaier, and R. Sigel, Phys. Rev. Lett. **39**, 1198 (1977).
[18]J.S. Pearlman, J.J. Thomson, and C.E. Max, Phys. Rev. Lett. **38**, 1397 (1977).
[19]P. Wagli and T.P. Donaldson, Phys. Rev. Lett. **40**, 875 (1978).
[20]B. Luther-Davies, Opt. Commun. **23**, 98 (1977).
[21]J.E. Balmer and T.P. Donaldson, Phys. Rev. Lett. **39**, 1084 (1977).
[22]B. Luther-Davies, Appl. Phys. Lett. **32**, 209 (1978).
[23]D.M. Villeneuve, G.D. Enright, and M.C. Richardson, Bull. Am. Phys. Soc. **22**, 1059 (1977).
[24]M.C. Richardson, N.H. Burnett, H.A. Baldis, G.D. Enright, R. Fedosejevs, N.R. Isenor, and I.V. Tomov, *Laser Interaction and Related Plasma Phenomena*, Vol. 4A, edited by H.J. Schwartz and H. Hora (Plenum, New York, 1977), p. 161.
[25]M.C. Richardson, R. Fedosejevs, P.A. Jaanimagi, and G.D. Enright, *Picosecond Phenomena*, edited by C.V. Shank, E.P. Ippen, and S.L. Shapiro (Springer-Verlag, Berlin, 1978), p. 274; P.A. Jaanimagi, N.R. Isenor, and M.C. Richardson, J. Opt. Soc. Am. **67**, 1404 (1977).
[26]These values were deduced from intensity distribution measurements made in the focal region at full laser power, utilizing Kalvar film as a threshold detector. These measurements are summarized in C. Joshi, G.D. Enright, and M.C. Richardson, NRC Internal Report, 1978 (unpublished).
[27]R. Fedosejevs, I.V. Tomov, N.H. Burnett, G.D. Enright, and M.C. Richardson, Phys. Rev. Lett. **39**, 932 (1977).
[28]G.D. Enright, N.H. Burnett, and M.C. Richardson, Appl. Phys. Lett. **31**, 494 (1977).
[29]G.D. Enright, M.C. Richardson, and N.H. Burnett, J. Appl. Phys. **50**, 3909 (1979).
[30]D.W. Forslund, J.M. Kindel, and K. Lee, Phys. Rev. Lett. **39**, 284 (1977).
[31]N.H. Burnett, H.A. Baldis, G.D. Enright, and M.C. Richardson, Appl. Phys. Lett. **31**, 172 (1977).
[32]N.H. Burnett, H.A. Baldis, G.D. Enright, and M.C. Richardson, Appl. Phys. Lett. **34**, 330 (1979); Bull. Am. Phys. Soc. **22**, 1077 (1977).
[33]D.M. Villeneuve, G.D. Enright, N. R. Isenor, and M.C. Richardson, Phys. Can. **33**, 33 (1977).
[34]I. Pelah, Phys. Lett. A **59**, 348 (1976).
[35]J.N. Olsen, G.W. Kuswa, and E.D. Jones, J. Appl. Phys. **44**, 2275 (1973).
[36]C. Joshi, G.D. Enright, and M.C. Richardson, Bull. Am. Phys. Soc. **23**, (October, 1978).
[37]B.H. Ripin, Appl. Phys. Lett. **30**, 134 (1977).
[38]S.R. Gunn and V.C. Rupert, Rev. Sci. Instrum. **48**, 1375 (1977).
[39]V. Cottles and D.V. Giovanielli, Los Alamos Scientific Laboratory Report LA-UR-77-1096, 1977 (unpublished).
[40]R. Fedosejevs, I.V. Tomov, G.D. Enright, and M.C. Richardson, Tenth Int. Quantum Electronics Conference, Atlanta, Georgia, 1978, paper I.9 (unpublished).